11th International Symposium on Magnetic Bearings
August 26-29, Nara, Japan

NUMERICAL SIMULATIONS AND EXPERIMENTS ON VIBRATION AT MAJOR CRITICAL SPEED OF ROTOR SUSPENDED BY MAGNETIC BEARING (INFLUENCE OF DECREMENT OF MAGNETIC FORCE DUE TO EDDY CURRENT CAUSED BY ROTATION)

Shin MURAKAMI
Shimane University, Nishikawatsu-cho 1060, Matsue, Shimane 690-8504 Japan
smurakam@riko.shimane-u.ac.jp

Takashi IKEDA
ibid.
tikeda@riko.shimane-u.ac.jp

Tsubasa WATANABE
Daido Castings Co., Ltd. Production Sect. Nagoya Plant, Ryugu-cho 10, Nagoya, Aichi 455-0022 JAPAN
TU-WATANABE@d-cast.jp

ABSTRACT
Vibration characteristic of a rotor supported by a PID controlled magnetic bearing is investigated. The differential equation of motion is derived with nonlinearities of the magnetic force for the gap, the current, and the characteristics of a current amplifier together with the decrement of magnetic force due to surface eddy current caused by rotation of the rotor. The influence of the rotational speed on the magnetic force is approximated by a fractional function and the coefficients are determined by experiments. By this approximation, the resonance curves for a major critical speed by the shooting method have good agreements with the experimental results.

INTRODUCTION
Recently, a lot of active magnetic bearings came into use in various fields. As a number of the magnetic bearings increase, the cases encountering failures or accidents, such as a large vibration by an unbalance due to some damage of a rotor, should also increase. Although a magnetic bearing has nonlinear properties in itself, most of them are controlled with linear control theory by linearization at equilibrium position. However, in the case above mentioned, the vibration phenomena should be considered with nonlinearities. There are many studies on the nonlinearity of magnetic bearings[1]-[9]. However, in these studies, the control parameters are not always applicable for real systems, for their aims are theoretical analyses such as bifurcation analysis. On the other hand, the authors have been comparing the theoretical analysis and the experimental results, considering the nonlinearity of the magnetic force. First, the static stiffness of a magnetic bearing was expressed as sum of polynomial components in polar coordinate system, which has regular shapes[10]. Then the effect of time delay of control force on the dynamic property of rotor system is clarified[11]. Later, some decrement of magnetic force that can't be explained by mere a time delay is found. We considered that this decrement is caused by the lag of magnetic flux due to eddy current on the rotor surface with rotation. We ascribe the decrement to the change of electromagnet constant. In this paper, we identify the relationship between the constant and rotational speed from the experimental results and verify the influence of the decrement by comparing the experimental resonance curve and the simulated one.

THEORETICAL ANALYSIS
Equation of motion
Figure 1 shows an analytical model for an experimental apparatus. A shaft is pivoted at its right hand. A disk is attached at right end of the shaft to verify the gyro effect. The shaft is suspended horizontally by a magnetic bearing with solid cylindrical rotor at its left end. Generally, laminating silicon steel is used in this part to suppress the eddy current. However, to a varying degree, it's impossible to suppress the eddy current completely especially in high-speed rotation. Therefore it is important to take an eddy current by rotation into account. The origin O of coordinate system is the geometrical center of magnetic bearing, and z-axis is set to the direction to the pivot P.

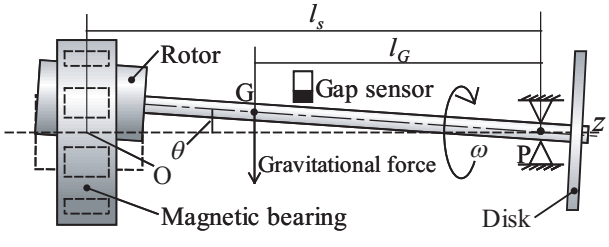

FIGURE 1: Analytical model

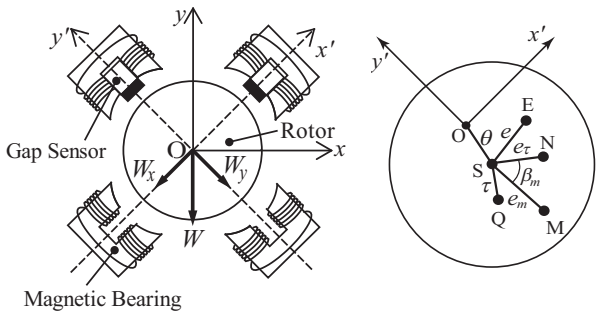

(a) Axis alignment (b) Unbalances

FIGURE 2: Cross section of magnetic bearing

Figure 2(a) shows the cross section of the magnetic bearing at O. To share the gravitational load to two control axes, the axes x' and y' are set to 45 deg incline from the vertical axis y. We assume that the push-pull and PID method is used to each axis independently each other.

To predict the vibration of rotor precisely, some kinds of unbalances must be considered, because there are inevitable errors on alignment of rotor, for example the error between the geometrical center at sensor position and that at magnetic bearing position. We consider the intersections of the O-$x'y'$ plane and the straight lines originating the pivot P. As shown in Figure 2 (b), we define the intersection of the line though the geometrical center of rotor at the sensor position as S, that of the geometrical center of rotor at the magnetic bearing as M, that of the gravitational center of rotor as E, and that of the principal axis of inertia as Q. Let the inclination of the shaft ($\angle$OPS represented by OS in Figure 2(b)) to be θ, the dynamic unbalance ($\angle$SPQ, represented by SQ) to be τ, and the angle corresponding the static unbalance (SE) to be e. We define the combination of the dynamic and static unbalance as the equivalent unbalance e_τ (SN) as follows.

$$e_\tau = \sqrt{(I_p - I)^2 + me\tau l_G (I_p - I)\cos\alpha + (mel_G)^2} \quad \cdots\cdots (1)$$

where I_p, I, m are the polar moment of inertia, the moment of inertia about gravitational center G, and the total mass of the rotor respectively, α is the phase difference between e and τ ($\angle$ESQ), l_G is the interval of the pivot P and the gravitational center G. Let the initial phase angle of e_τ is zero and the projectile angles of θ to the O-$x'z$ and O-$y'z$ plane to be θ_x and θ_y respectively. The equation of motion of the rotor is derived as

$$\left.\begin{aligned}(I + ml_G{}^2)\ddot{\theta}_x + I_p\omega\dot{\theta}_y &= \\ -M_{\theta x} + e_\tau\omega^2\cos\omega t - W_x l_G& \\ (I + ml_G{}^2)\ddot{\theta}_y - I_p\omega\dot{\theta}_x &= \\ -M_{\theta y} + e_\tau\omega^2\sin\omega t - W_y l_G&\end{aligned}\right\} \cdot (2)$$

where $W_x l_G$, $W_y l_G$ are the x' and y' components of the moment due to gravitational force. $M_{\theta x}$ and $M_{\theta y}$ are the restoring moments by the magnetic bearing. In this section, we consider the ideal case, in which no eddy current and no time lag of magnetic flux exist. After some calculations, the restoring moments can be represented as follows.

$$\left.\begin{aligned}M_{\theta x} = l_m k\Bigg[&\left\{\frac{I_b(1-w_x)+i_x}{H+l_m(\theta_x+e_m\cos(\omega t+\beta_m))}\right\}^2 \\ &-\left\{\frac{I_b(1+w_x)-i_x}{H-l_m(\theta_x+e_m\cos(\omega t+\beta_m))}\right\}^2\Bigg] \\ M_{\theta y} = l_m k\Bigg[&\left\{\frac{I_b(1-w_y)+i_y}{H+l_m(\theta_y+e_m\sin(\omega t+\beta_m))}\right\}^2 \\ &-\left\{\frac{I_b(1+w_y)-i_y}{H-l_m(\theta_y+e_m\sin(\omega t+\beta_m))}\right\}^2\Bigg]\end{aligned}\right\} \quad (3)$$

where l_m is the interval of the pivot P and the geometrical center of the magnetic bearing O. The load ratio w_x, w_y are defined as $w_x = W_x l_G/(W_0 l_m)$, $w_y = W_y l_G/(W_0 l_m)$, where $W_0 = k(2I_b/H)^2$, H is the gap of the magnetic bearing and I_b is the average bias current. The control currents i_x, i_y are defined as

$$\left.\begin{aligned}i_x &= k_{px}\theta_x + k_{dx}\dot{\theta}_x + k_{ix}\int\theta_x dt \\ i_y &= k_{py}\theta_y + k_{dy}\dot{\theta}_y + k_{iy}\int\theta_y dt\end{aligned}\right\} \quad \cdots\cdots\cdots\cdots (4)$$

where k_{px}, k_{py}, k_{dx}, k_{dy}, k_{ix}, k_{iy} are the proportional, differential, integral gains of x' and y'-axis of PID control. In this paper, the load ratio and the feedback gains are assumed to be same in both axis, i.e., $w_x = w_y = w$, $k_{px} = k_{py} = k_p$ and so on.

Vanishing the unbalances e_τ, e_m, the differential and integral gains k_d, k_i and rotational frequency ω, and linearizing Eq.(2) with Eq.(3) and Eq.(4), we can obtain the natural frequency of the system ω_n as

$$\omega_n = \frac{2I_b}{H}\sqrt{\frac{kl_m^2}{I+ml_G^2}\left(\frac{k_p}{I_b} - \frac{1+w^2}{H}\right)}. \quad \cdots\cdots\cdots (5)$$

We introduce following dimensionless variables and parameters.

$$\theta_x' = \frac{l_m}{H}\theta_x,\ \theta_y' = \frac{l_m}{H}\theta_y,\ t' = \omega_n t,\ i_p' = \frac{I_p}{I+ml_G^2},\ \omega' = \frac{\omega}{\omega_n},$$
$$k' = \frac{l_m^2 I_b^2}{\omega_n^2 H^3(I+ml_G^2)}k,\ k_p' = \frac{H}{I_b}k_p,\ k_d' = \omega_n\frac{H}{I_b}k_d$$

Hereafter, the symbol "$'$" for dimensionless quantity is omitted. Using these representations, we get the dimensionless equation of motion as follows.

$$\left.\begin{aligned}\ddot{\theta}_x + i_p\omega\dot{\theta}_y &= -M_{\theta x} + e_\tau\omega^2\cos\omega t - \frac{w}{k_p - w^2 - 1} \\ \ddot{\theta}_y - i_p\omega\dot{\theta}_x &= -M_{\theta y} + e_\tau\omega^2\sin\omega t - \frac{w}{k_p - w^2 - 1}\end{aligned}\right\} \cdot (6)$$

The dimensionless restoring moments by magnetic bearing M_{θ_x}, M_{θ_y} in Eq.(6) are represented as follows

$$\left.\begin{aligned} M_{\theta_x} &= k\left[\left\{\frac{(1-w)+i_x}{1+(\theta_x+e_m\cos(\omega t+\beta_m))}\right\}^2 \right. \\ &\quad \left. -\left\{\frac{(1+w)-i_x}{1-(\theta_x+e_m\cos(\omega t+\beta_m))}\right\}^2\right] \\ M_{\theta_y} &= k\left[\left\{\frac{(1-w)+i_y}{1+(\theta_y+e_m\sin(\omega t+\beta_m))}\right\}^2 \right. \\ &\quad \left. -\left\{\frac{(1+w)-i_y}{1-(\theta_y+e_m\sin(\omega t+\beta_m))}\right\}^2\right] \end{aligned}\right\} \quad (7)$$

From the linearized equations of Eq.(6) and Eq.(7), the equivalent damping ratio $\zeta = 2kk_d$.

Discussion on magnetic force

To predict the practical case, the property of monopole current amplifier and the time delay of the control current must be considered. Additionally, we consider the decrement of magnetic force due to eddy currents by rotation.

The contents of $\{\}$ in the right hand side of Eq.(7) represent the dimensionless values correspond to (current/gap). These values are proportional to the magnetic flux density, hence we define these are the dimensionless magnetic flux densities $\bar{B}_{mx}$, $\bar{B}_{px}$ as follows (we discuss only about θ_x direction here, because θ_y can be regarded as similar).

$$\bar{B}_{mx} = \left\{\frac{\max((1-w)+i_x,0)}{1+(\theta_x+e_m\cos(\omega t+\beta_m))}\right\} \quad \cdots\cdots\cdots (8)$$

$$\bar{B}_{px} = \left\{\frac{\max((1+w)-i_x,0)}{1-(\theta_x+e_m\cos(\omega t+\beta_m))}\right\} \quad \cdots\cdots\cdots (9)$$

The subscript $_m$ represents the gap in the negative axis direction, and $_p$ in the positive one. Because the monopole current amplifier can run the current to only one direction, if a numerator becomes less than zero, it is forced to be vanished.

There is a time lag in current in fact, so we assume this is first-order lag and let the time constant as T. The dimensionless magnetic flux densities becomes as

$$B_{mx} = \bar{B}_{mx} - T\dot{B}_{mx} \quad \cdots\cdots\cdots\cdots\cdots\cdots\cdots (10)$$

$$B_{px} = \bar{B}_{px} - T\dot{B}_{px} \quad \cdots\cdots\cdots\cdots\cdots\cdots\cdots (11)$$

and the moments are represented as

$$M_{\theta_x} = k\left(B_{mx}^2 - B_{px}^2\right) \quad \cdots\cdots\cdots\cdots\cdots\cdots\cdots (12)$$

Similarly, we can obtain

$$M_{\theta_y} = k\left(B_{my}^2 - B_{py}^2\right). \quad \cdots\cdots\cdots\cdots\cdots\cdots\cdots (13)$$

Figure 3 shows a development of a magnetic bearing and a rotor surface. The variation of magnetic flux density at point A on the rotor surface which moves from left side toward right side with rotation as illustrated. Because of the existence of eddy currents, the density varies as the solid curve with the movement of point A. As a result, the attractive magnetic forces incline as the slanted arrows. The restoring force of the magnetic bearing is the sum of the vertical components of theses forces, therefore the force decreases as rotational speed increases. We consider this decrement changes the electromagnetic constant k, and treat it as the function of angular velocity of rotor $k(\omega)$. Assuming the averaged moment and gravitational moment are balanced, we can identify $k(\omega)$ from the time histories of currents and air gaps in experiment and the static load at the bearing, because the unbalance force vanishes by averaging with time. Therefore we get the balancing equation as follows

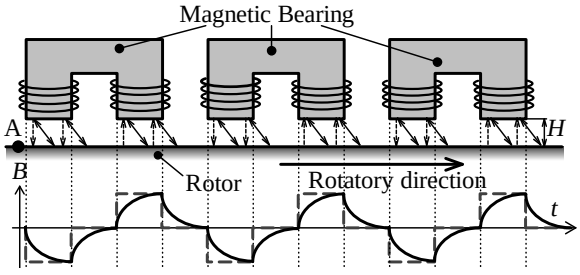

FIGURE 3: Effect of rotational speed on magnetic flux density

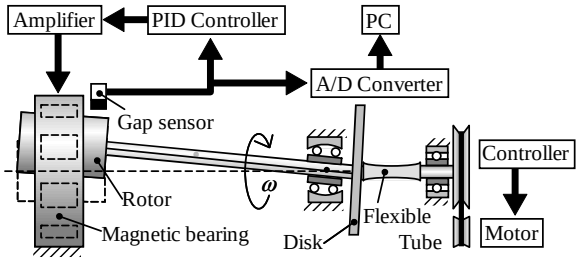

FIGURE 4: Experimental apparatus

$$l_m k(\omega)\left\{\overline{\left(\frac{I_{x+}}{H-x}\right)^2} - \overline{\left(\frac{I_{x-}}{H+x}\right)^2}\right\} = W l_G \quad \cdots (14)$$

I_{x+}, I_{x-} are the electromagnet current and x is the displacement of the rotor. The symbol "—" means the averaging with time. In this calculation, the error e_m is assumed to be sufficiently smaller than the displacement.

EXPERIMENTAL RESULTS AND SIMULATION

Figure 4 shows the outline of the experimental apparatus. A shaft of length about 405 mm is supported by a self-aligning ball bearing at right hand as pivot and supported by magnetic bearing at left end. An electromagnetic stainless cylindrical rotor of diameter 68 mm is attached to the shaft. A disk is attached the right end

TABLE 1: Specification of experimental apparatus

Gap H	0.33	mm
Total mass of shaft m	10.04	kg
Position of gravitational center l_G	67.96	mm
Position of magnetic bearing l_m	364.5	mm
Polar moment of inertia I_p	0.0525	kgm^2
Moment of inertia $I+ml_G^2$	0.415	kgm^2

of the shaft. A rotating torque of motor is transmitted through pulleys and a flexible tube. The PID controller consists of analog OP amp circuits. Electromagnetic currents are supplied by monopole current amplifier. The time histories of shaft displacement and electromagnetic currents are measured by computer-based measurement system with sampling frequency 10 kHz and 16-bit resolution. The apparatus contains a touch down bearing to avoid destruction. It limits the amplitude of shaft to about 0.15 mm at magnetic bearing position, 0.5 in dimensionless representation. Other specifications are listed in Table 1.

Effect of rotating speed on magnetic constant

The magnetic force constant is obtained by Eq.(14) with the experimental time histories of the currents and the gaps at various rotational speed. Figure 5 shows an example of time histories of displacement and currents.

The standard values of control parameters are chosen as follows. The load ratio $w = 0.25$, the equivalent damping ratio $\zeta = 0.5$, and the dimensionless integral feedback gain $k_i = 0.05$. These parameters are determined by the electric circuits of PID controller. Figure 6 shows the magnetic force constant vs rotational speed. They are for the dimensionless proportional feedback gain k_p =1.8, 2.0, 2.2. The broken curves are the approximation with a fractional function form as

$$k(\omega) = \frac{k_\alpha}{k_\beta + \omega} + k_\gamma. \quad \cdots\cdots\cdots\cdots\cdots\cdots\cdots\cdots (15)$$

The parameters k_α, k_β, k_γ can be determined by the least square method with the experimental data. This figure shows the dimensionless proportional feedback gain k_p has little influence on the magnetic force coefficient $k(\omega)$. Since the obtained function has a real dimension, we take it into account to the equation of motion after appropriate nondimensionalization.

Resonance curve at major critical speed

Figure 7 shows the resonance curves obtained by experiments in the vicinity of major critical speed . The standard values of the control parameters are the same as previous section. The symbol "$\circ$" and "$\bullet$" indicate the displacement amplitude at magnetic bearing in x'-axis and y'-axis direction, respectively. In previous papers

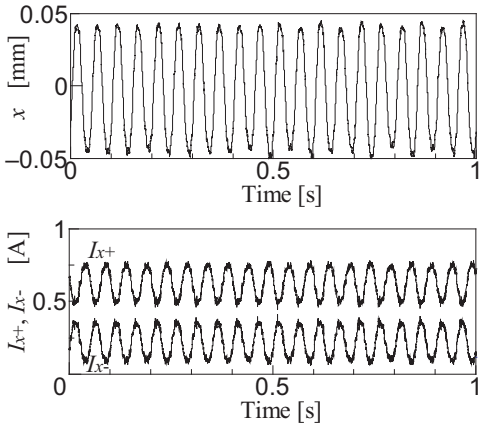

FIGURE 5: Time history of displacement and current

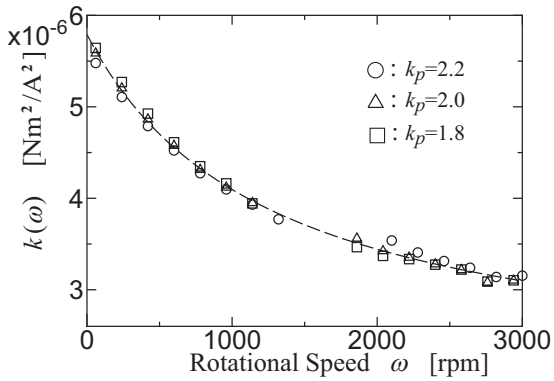

FIGURE 6: Variation of the electromagnetic constant

[10],[11], it is known that the resonance curve of most magnetic bearing system becomes soft spring type. We can confirm there's slightly tendency to be softening of the resonance curve, though it is unclear because of the amplitude limitation by a touch down bearing.

In the steady state solution analysis for a nonlinear vibration problem, the harmonic balance method, a kind of approximation method, is often used[11]. However, this method needs to express the nonlinearity in polynomial function and its procedure is cumbersome. While a direct numerical simulation of the equation of motion without approximation is a time consuming process because it needs long time to reach steady state solution. In addition, this has another disadvantage that can't obtain unstable solution. Therefore we choose the shooting method[12] to obtain the steady state solution.

In Figure 7, the solid line represents the resonance curve of proposed method (with consideration of decrement of magnetic force by Eq.(15)), and the broken line is that of previous method (with electromagnetic force constant k =Const.). In this calculation, the parameters $e_\tau = 0.1$, $e_m = 0.06$, $T = 0.7$, $\beta_m = \pi/2$ are identified by

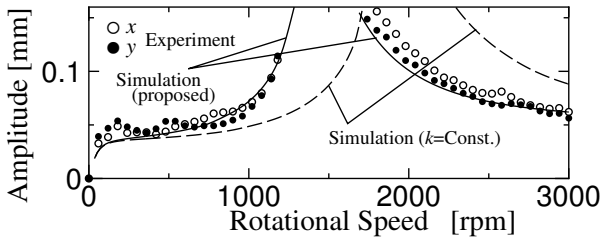

(a) $k_p = 1.8$

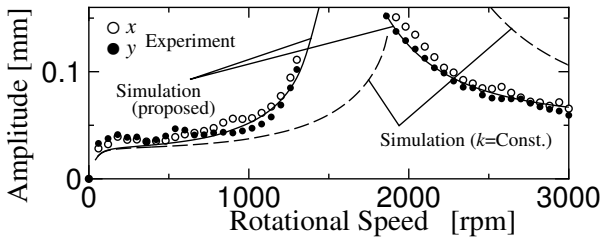

(b) $k_p = 2.0$

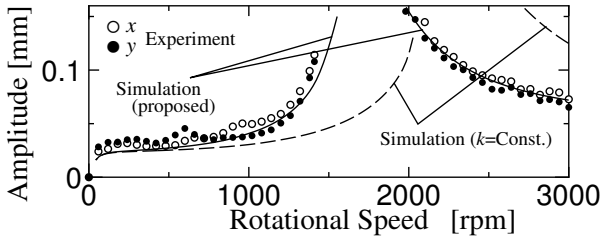

(c) $k_p = 2.2$

FIGURE 7: Resonance Curves

curve fitting. These data are calculated in dimensionless form first, and later transferred to real dimensions. Comparing the experimental data and the simulation results of proposed method and previous method, we can see the validity of proposed method.

CONCLUTION

The vibration characteristics of a rotor supported by a magnetic bearing in the vicinity of major critical speed are investigated with consideration of the decrement of the electromagnetic force with the rotational speed. Following results are obtained:

(1) The variation of the electromagnetic force can be formulated by averaging the calculated instant force from displacement and current data obtained by experiment.

(2) The resonance curves become soft spring type because of nonlinearity of magnetic force.

(3) The resonance curves have good agreements with the experimental results by consideration of the decrement of the electromagnetic force with the rotational speed.

REFERRNCES

1. J. D. Knight and H. Ecker, Simulation of Nonlinear Dynamics in Magnetic Bearing, *Proc. of Computer Simulation Conf.*, Portland, (1996)

2. M. Chinta and A. B. Palazzolo, Stability and Bifurcation of Rotor Motion in a Magnetic Bearing, *J. of Sound and Vibration*, Vol. 214, No.5 (1998), pp.793-803

3. N. Steinschaden and H. Springer, Some Nonlinear Effects of Magnetic Bearings, *Proc. of DETC ASME Conf.*, Las Vegas, VIB-8063, (1999)

4. J. C. Ji et al., Bifurcation Behaviour of a Rotor Supported by Active Magnetic Bearing, *J. of Sound and Vibration*, Vol. 235, No.1 (2000), pp.133-151

5. J. C. Ji and C. H. Hansen, Non-linear Oscillations of a Rotor in Active Magnetic Bearing, *J. of Sound and Vibration*, Vol. 240, No.4 (2001), pp.599-612

6. J. C. Ji and A. Y. T. Leung, Non-linear Oscillation of a Rotor-Magnetic Bearing System Under Superharmonic Resonance Conditions, *Int. J. of Non-linear Mechanics*, Vol. 38, No.6 (2003), pp.829-835

7. J. C. Ji, Dynamics of a Jeffcott Rotor-Magnetic Bearings System with Time Delay, *Int. J. of Non-linear Mechanics*, Vol. 38, No.9 (2003), pp.1387-1401

8. J. C. Ji, Stability and Hopf Bifurcation of a Magnetic Bearing System With Time Delays, *J. of Sound and Vibration*, Vol. 259, No.4 (2003), pp.845-856

9. Y. S. Ho et al., Effect of Thrust Magnetic Bearing on Stability and Bifurcation of a Flexible Rotor Active Magnetic Bearing System, *Trans. of ASME J. of Vib. and Acoust.*, Vol. 125, No.3 (2003), pp.307-316

10. S. Murakami et al., Nonlinear Characteristics of Restoring Force due to a Magnetic Bearing, *Journal of the JSAEM*, Vol. 13, No.1 (2005), pp.71-76(in Japanese)

11. T. Inoue et al., Theoretical Analysis and Experiments of the Nonlinear Vibration in a Vertical Rigid Rotor supported by the Magnetic Bearing System (Case Considering the Delay of Control Force), *Journal of System Design and Dynamics*, Vol. 1, No.2, pp.295-306

12. H. Tamura and K. Matsuzaki, Numerical Scheme and Program for the Solution and Its Stability Analysis for a Steady Periodic Vibration Problem, *Trans. of JSME, Ser.C*, Vol. 60, No.569 (1994), pp.30-37 (in Japanese)